APPLIED
MATERIALS
AND TECHNOLOGY

Research Article

Jamt.ejournal.unri.ac.id

Synthesis of Calcium Silicate Hydrate Compounds from Wet Flue Gas Desulfurization (FGD) Waste

Denise Alves Fungaro, Lucas Grosche and Juliana de C. Izidoro*

Instituto de Pesquisas Energéticas e Nucleares, IPEN-CNEN/SP, 05508-000, Brazil

ABSTRACT: In this study Calcium silicate hydrate based products (CSHP) were synthesized from wet flue gas desulfurization waste (FGD) by alkali fusion followed by hydrothermal treatment. The effect of various factors on the formation of products, such as mineralizing agent, fusion temperature and time, crystallization time and addition of Ca and Si were studied as well as the conditions optimized. The FGD and synthesized materials were characterized by using X-Ray (XRD), Scanning Electron Microscope (SEM), X-ray fluorescence (XFR), among other methods. A fusion temperature of 600 °C with NaOH, fusion duration of 1 h, and a subsequent hydrothermal temperature of 100 °C for a reaction of 24 h were found to be the optimal conditions. In these synthesis conditions, CSHP containing tobermorite and Al-tobermorite was the major phases. The synthesized CSHP revealed high selective uptake for Cs^+ in water. The maximum adsorption capacity of Cs^+ onto the synthesized material, as calculated from the Langmuir model, was 1949 μmol g^{-1}. The performance on the Cs^+ removal in the presence of high Na^+ contents was also evaluated. The adsorbent material showed a high Cs^+ adsorption capacity in deionized water and a decrease of 56% and 62% in saturated media with the Na^+ ions and seawater, respectively. Therefore, CSHP as a higher value-added product can be obtained from a by-product of a coal-fired power plant, which has wide range applications, including for Cs^+ removal from wastewater.

Key words: Flue Gas Desulfurization waste; Alkaline hydrothermal conversion; Hydrated calcium silicate; Cs (I) removal.

1. INTRODUCTION

The development of the generation of electricity in nuclear power plants, nuclear weapons testing, and the use of radionuclides in research and medicine have led to the increase production of radioactive waste materials and their release into the environment.

In 2011 due to the nuclear power plant accident at Fukushima Daiichi in Japan large amount of radioactive materials were released into the atmosphere, as a result of which the surface water and soil particles were severely contaminated [1].

Among the several nuclides, ^{137}Cs is considered to be the most harmful among the fission product nuclides since it has an intermediate half-life time (30.17 years), decays by high-energy pathways, and possesses high solubility and chemical reactivity [2]. Therefore, it is extremely important to choose a suitable and effective method to remove cesium from aqueous systems. The physical and chemical characteristics of cesium ion make it difficult to be separated from aqueous solutions containing Na^+ and K^+ due to their homologous behavior.

Different methods such as ion exchange, precipitation, solidification, and stabilization can be applied for remediation or treatment of soil and water contaminated by Cs^+. Among them, ion exchange using different materials is the most studied. Much attention has been focused on the uptake of Cs^+ on zeolites, clay minerals, and other adsorbents [3, 4].

Calcium silicate hydrate (CSH) compound has shown excellent potential in the safe disposal of low and intermediate-level radioactive waste [5]. Tobermorite is the most important compound in various CSH and can act as a cation exchanger. Aluminum-substituted 11 A tobermorite (Al-tobermorite), in particular, shows high cation exchange and high selectivity for Cs^+, including in solution with high concentrations of sodium [6].

The synthesis of tobermorite compounds in various conditions has been extensively studied using analytical grade reagents. Generally, Ca^{2+} and SiO_2 react to form C–S–H phases under hydrothermal conditions [7], [8]. Under different hydrothermal conditions, varieties of CSH with different structures can be prepared [9].

The synthesis of CSH compounds can also be performed with by-products under hydrothermal treatment, such as newsprint recycling residue, municipal waste incineration fly ashes, oil shale ash, cement bypass dust, coal fly ash, waste container glass, etc. [10 - 12].

On the other hand, the large amount of by-products produced from wet flue gas desulfurization technology in coal-fired power stations results in massive accumulation of flue gas desulfurization (FGD) gypsum, which triggers a series of environmental problems [13]. Therefore, the conversion from FGD gypsum to high value-added materials can bring both economic and environmental benefits.

Thus, this study aimed to evaluate the synthesis of calcium silicate hydrate based products containing

Received : April 13, 2020
Revised : April 25, 2020
Accepted : May 09, 2020

tobermorite and Al-tobermorite from the FGD and its removal ability of Cs(I) from aqueous solution was estimated to apply for treatment of the environmental contamination with radioactive Cs^+. Also, the interaction mechanism between adsorbate and adsorbent at equilibrium time was explored by Freundlich and Langmuir models.

2. MATERIALS AND METHODS

2.1 Materials

All chemicals that are used in this study were of analytical grade. The waste produced from the wet flue gas desulfurization process (FGD) was collected at the Presidente Médici Thermoelectric Power Plant (located in Rio Grande do Sul state, Brazil). Silica synthesized from ashes from sugarcane residue [14] and $Ca(OH)_2$ (Sigma-Aldrich) were used in the study. Besides, deionized water was used in all experiments.

2.2 Methods

In the first step, 10 g of FGD ash was mixed with 12 g of a mineralizing agent (NaOH or $Ca(OH)_2$). The grinded mixture was heated in a muffle furnace at different times and temperatures. After the cooling at room temperature, 100 mL of deionized water was added to the mixture and the product was then stirred for 18 h and heated to 100 °C in an oven at different times. The suspension was then filtered and the solid was repeatedly washed with deionized water until pH ~10 and dried at 100 °C for 24 h.

Studies have shown that NaOH is an optimal mineralizing agent, which favors the dissolution of the crystalline phases of ashes during fusion at different temperatures, such as 600 °C. On the other hand, the dissolution of mullite and quartz is more difficult with calcium hydroxide, therefore requiring higher temperatures. XRD patterns in preliminary studies showed significant crystalline of phases of ashes at 600 °C with $Ca(OH)_2$, which results in a low yield of the final product, and so this temperature was not considered in the study.

In a second test, 0.7 g of silica and 1.4 g of $Ca(OH)_2$ were mixed with NaOH at the fusion step in order to adjust the molar ratio of Si/Al/Ca. That adjustment aimed to reach the specifical molar ratio suitable to the synthesis of Al-tobermorite according to the literature [15 - 17]. The amount of 0.7 g of silica was added to the samples in which calcium hydroxide was used as a mineralizing agent.

In a third test, the fusion step was carried out at temperatures of 800 °C and 900 °C and without a mineralizing agent. The intention at this stage was to evaluate the necessity of the mineralizing agent, and if solubilization of the crystalline phases would take place by only increasing the temperature at the fusion step of the synthesis. Experimental conditions of synthesis of calcium silicate hydrate based products (CSHP) are shown in Tab. 1.

2.3 Characterization of Materials

Samples were characterized in terms of chemical composition by X-ray fluorescence (Rigaku – RIX 3000). A scanning electron microscope was used to verify the morphology of the samples (Philips XL 30). The mineralogical composition was determined by X-ray diffraction (Rigaku – Multiflex) using Cu Kα radiation at 40 kV and 20 mA.

The particle size distribution for the samples was determined using a laser diffraction particle size analyzer (Malvern – Mastersizer 2000). The pH measurements were done by using a shaking table (Ética - 430), a shaker machine (Orbital Shaker incubator – SF-670) and a pH meter (MS Tecnopon - MPA 210 / TPS – WP-81). The real density of samples was determined by a helium pycnometer

Table 1 Experimental conditions of the fusion process for CSHP synthesis

Sample	Mineralizing Agent	Fusion		Crystallization Time (h)	Ca/Si addition
		T (°C)	t (h)		
CSHP-1	no	900	1	0	yes
CSHP-2	no	900	1	24	yes
CSHP-3	no	800	1	0	yes
CSHP-4	no	800	1	24	yes
CSHP-5	Ca(OH)2	750	3	0	yes
CSHP-6	Ca(OH)2	750	3	24	yes
CSHP-7	Ca(OH)2	750	3	48	yes
CSHP-8	Ca(OH)2	750	3	72	yes
CSHP-9	NaOH	750	3	0	yes
CSHP-10	NaOH	750	3	24	yes
CSHP-11	NaOH	750	3	48	yes
CSHP-12	NaOH	750	3	72	yes
CSHP-13	NaOH	600	1	24	no
CSHP-14	NaOH	600	1	24	yes
CSHP-15	NaOH	600	3	24	no

pycnometer (Micromeritcs Instrument Corporation - Accupyc 1330).

In cation exchange capacity (CEC) measurements, 1 g of each sample was saturated with 100 mL of sodium acetate solution (1 mol L^{-1}), washed with 1 L of distilled water, dried, and then mixed with 100 mL of ammonium acetate solution (1 mol L^{-1}). The sodium ion concentration of the remaining solution was determined by inductively coupled plasma optical emission (ICP-OES – Spectro - Arcos).

Three titrant solutions were used to evaluate the pH changes by using the zeta potential (two acidic solutions of HNO_3 0.025 and 0.25 mol L^{-1} and an alkaline solution of NaOH 0.25 mol L^{-1}. The pH ranges studied were between 2 and 12, varying from 1 to 1. All solutions were prepared with MilliQ water. The equipment used for the measurements was the Zetasizer Nano ZS-90 with a multi-purpose MPT2 titrator (Malvern Instruments - Multipurpose Titrator).

2.4 Cesium adsorption studies

2.4.1 Adsorption isotherms

Batch processes for cesium adsorption were performed by shaking 0.05 g of adsorbent material and 10 mL of cesium chloride and ^{137}Cs (used as a radioactive tracer for the measurements) solutions with different and known initial concentrations.

A stock solution of ^{137}Cs was prepared from a standard solution of 1 mCi mL^{-1} (20 µL of the standard solution were used to prepare 1 mL of the stock solution).

The solutions with concentrations ranging from 100-6000 µmol L^{-1} of CsCl and containing 10 µL of the ^{137}Cs tracer stock solution were prepared. The adsorbent material and the cesium solutions were stirred at 120 rpm for 24 h and room temperature. Then, the supernatants were separated from the adsorbent by centrifugation and the concentrations were determined by a gamma spectrometer (HPGe - GX1518) coupled to a multichannel acquisition system (Canberra Inc.). Tests were performed in duplicate for each concentration of Cs.

The interaction mechanism between adsorbate and adsorbent at equilibrium time was explored by Freundlich and Langmuir models [18, 19]. The Chi-square (c^2) test was employed, the lowest values were used to validate the applicability of isotherms tested [20].

2.4.2 Adsorption studies in saline medium

Cesium adsorption studies were carried out from two different saline matrices: one containing a solution of NaCl (0.02 mol L^{-1}) and the other containing a sample of real seawater, collected in Santos coast, located in São Paulo State, Brazil. Real seawater was filtered before the tests.

All tests were performed with Cs^+ solutions with $2x10^{-4}$ mol L^{-1} of concentration and ^{137}Cs as a radioactive tracer. The adsorbent material and the saline cesium solutions were stirred at 120 rpm for 24 h at room temperature. Then, the concentrations were determined in the similar way as in the adsorption isotherms procedure. Tests were performed in triplicate.

The amount of the Cs^+ uptake and percentage of Cs^+ removal by the adsorbent were calculated by applying eqn (1) and (2), respectively, where q is the adsorbed amount of adsorbate per gram of adsorbent (µmol g^{-1}), C_0 and Ct are the concentrations of the adsorbate in the initial solution, and at any time (t), respectively (mg L^{-1}), V is the volume of the adsorbate solution added (L) and M is the amount of the adsorbent used (g).

$$q = \frac{V(C_0 - C_t)}{M} \quad (1)$$

$$R = \frac{100\,(C_0 - C_t)}{C_0} \quad (2)$$

Distribution coefficient Kd, signifying the affinity and selectivity for Cs+, was calculated by the eqn (3), where Ci and Ce are the initial and final concentrations of Cs+ (mg L-1), V is the volume of the tested solution (L), and m is the weight of the adsorbent (g).

$$Kd = [(Ci - Ce)/Ce] \times (V/m) \quad (3)$$

3. RESULTS AND DISCUSSION

3.1. Characterization of FGD

3.1.1 Chemical composition

The chemical composition of FGD waste obtained by X-ray fluorescence is given in Tab. 2, and shows that the major constituents were silica, alumina, and calcium, iron and sulfur compounds. The high magnesium content is justified because in the wet process Mg^{2+} is used to improve the oxidation efficiency of coal combustion products, thus increasing the amount of magnesium sulfate produced. The percentage of FGD elements is within the range usually encountered in this type of residue and reported in the literature [21].

Table 2 Chemical composition (wt%) of FGD waste

Components	FGD
CaO	26.3
SiO_2	22.2
MgO	13.4
SO_3	11.2
Al_2O_3	6.76
Fe_2O_3	2.39
K_2O	0.873
TiO_2	0.328
MnO	0.026
CoO	0.024
WO_3	0.023
SrO_2	0.022
V_2O_5	0.014
ZrO	0.014
ZnO	0.009
Others	<0.001
LOI	16.3

3.1.2 Mineralogical composition

Fig. 1 shows X-ray diffraction patterns (XRD) of the FGD sample, and the respective crystalline phases are identified in Tab. 3. The sample presented an ettringite phase (which contains calcium and sulfate in its structure) and brucite phase, which are commonly found in residues from the process of wet desulfurization [22].

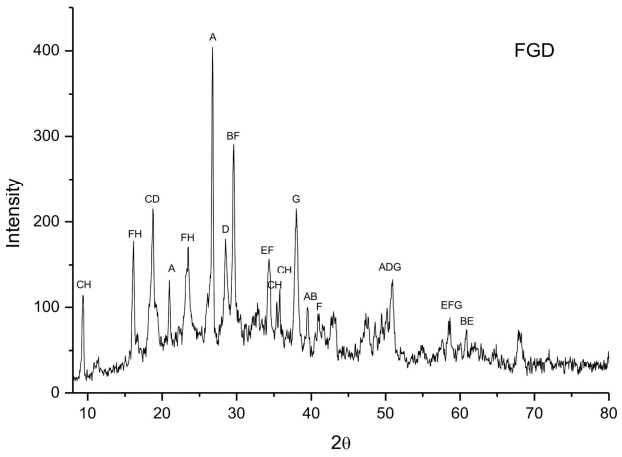

Fig. 1. XRD Pattern of FGD waste (A = Quartz, B = Calcite, C = Chabazite, D = Portlandite, E = Sodium carbonate, F = Brucite , G = Ettringite and H = Hydrated hydroxide of calcium oxide and aluminum).

Table 3 Mineralogical composition of FGD waste

Compound	Formula
Quartz	SiO_2
Calcite	$CaCO_3$
Chabazite	$Ca_{1.979}Al_{3.8}Si_{8.2}O_{24}$
Portlandite	$Ca(OH)_2$
Sodium carbonate	Na_2CO_3
Brucite	$Mg(OH)_2$
Ettringite	$Ca_6Al_2(SO_4)(OH)_{12}.26H_2O$
Hydrated hydroxide of calcium oxide and aluminum	$Ca_6Al_2O_6(OH)_6.32\ H_2O$

3.1.3 Particle size distribution

Fig. 2 reports the differential and cumulative particle size distributions for FGD. The differential size distribution of the material is relatively uniform with the expected normal bell-shaped distribution curve. The particle size distributions of material are given in Tab. 4. These distributions specify that the majority of particles (90%) lie below 192 μm. It was reported that gypsum from full-scale plants present d_{50} around 34.9 μm [23]. The $D_{3,2}$ diameter value, calculated by the equipment, is based on the average surface area of the particles and usually is used to design particle retention equipment. The $D_{3,2}$ and D_{90} values found in this study is in accordance with the values found for similar wastes reported in the literature [24].

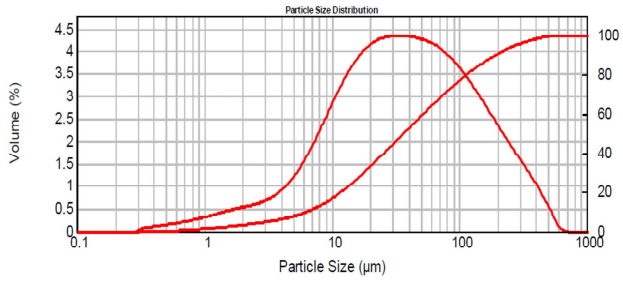

Fig. 2. Particle size distribution of FGD waste.

Table 4 Particle size distribution of FGD waste

Parameter	Particle diameter
D_{10} (μm)	6.273
D_{50} (μm)	36.734
D_{90} (μm)	191.812
$D_{(3.2)}$	11.527

3.1.4 Morphological characterization

The scanning electron micrographs (SEM) of the FGD waste are shown in Fig. 3. The FGD sample presented heterogeneous particles with different diameters and shapes. Smooth surface spheres are usually silico-aluminous compounds, whereas irregular shapes particles are usually unburnt coal, magnetic particles of iron oxide, amorphous particles which suffered a rapid cooling, or other types of minerals. In addition to the structures already mentioned, a large presence of chabazite, brucite and rhombohedral crystals can be observed in Fig. 3(b) [25].

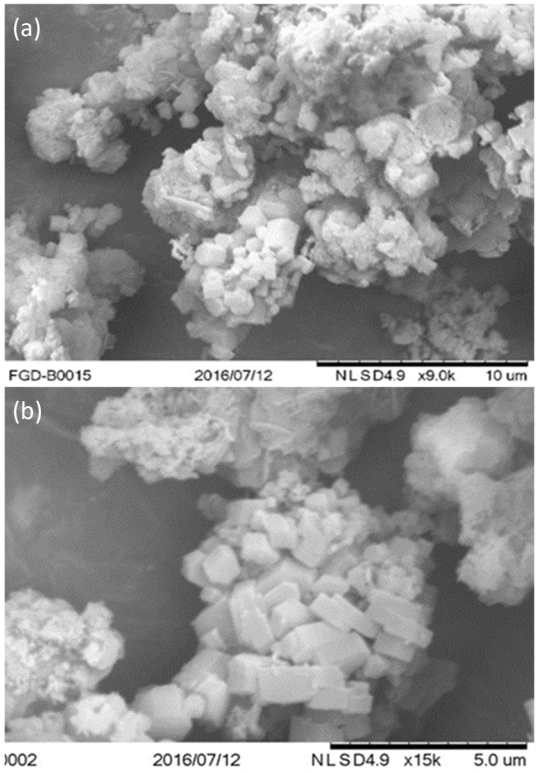

Fig. 3. SEM micrographs of FGD waste sample (a) expanded by 9000X; (b) expanded by 15.000X.

3.1.5 Physicochemical properties

The physical and chemical properties of the FGD sample are shown in Tab. 5. The real density values are in accordance with literature which establishes that materials with the presence of crystalline phases such as mullite and quartz present density between 2.0 to 2.5 g cm^{-3} [26].

According to Kost et. al [27], the pH of the FGD residues depends first on the adsorbent used during the desulfurization process (usually calcite, dolomite or calcium hydroxide) and then on the type of technology. The authors concluded that the high pH value for most residues is due to the presence of Ca and Mg oxides and hydroxides. When products are exposed to water and CO_2, they are converted

to carbonates by carbonation reactions and as a consequence, the pH value of the aqueous solution increases. Usually, this type of waste has a pH range of 9 to 14. The residue may also contain an excess of alkaline adsorbent that did not react with SO_2 during the coal combustion [27]. Samples of silicon-aluminous coal ash from different Brazilian thermoelectric plants showed CEC values very close to those found for the FGD residue [28].

Table 5 Physicochemical properties of FGD waste

Characteristic	Values
Real density (g cm^{-3})	2.34
pH	11.7
Cation Exchange Capacity (CEC) (meq g^{-1})	0.022

3.2 Characterization of synthesized products from FGD

The composite microstructure of CSHP was firstly examined considering the formation of crystalline phases. In the set of experiments by using 900 °C and 800 °C without a mineralizing agent (Tab. 1, CSHP-1-4), the XRD patterns of the products (not shown) indicated the formation of several complex crystalline structures of Ca-Si-Al type, mainly prehnite ($Ca_2Al_2Si_3O_{10}(OH)_2$) and gehlenite ($Ca_2Al_2SiO_7$), on the other hand, tobermorite compounds were not obtained. The process resulted in a solid-solid reaction and, once the crystalline structures were formed during the fusion, there was only an intensification of the reaction during the hydrothermal treatment process.

In the second set of experiments, $Ca(OH)_2$-activation experiments were carried out at 750 °C (Tab. 1, CSHP-5-8), and the XRD patterns of the products (not shown) indicated the formation of portlandite ($Ca(OH)_2$) as the main phase, and compounds of alumino-silicates and calcium silicates in lesser quantity when compared to the other phases. There was no influence on the crystallization time. The sample that was not subjected to the hydrothermal treatment (Tab. 1, CSHP-5) also showed the presence of quartz (SiO_2), periclase (MgO), and calcium oxide (CaO). These compounds were in the raw material as hydrated form and remained in the products after the synthesis (they were only dehydrated).

In the set of experiments carried out with the fusion process at 750 °C and NaOH as a mineralizing agent (Tab. 1, CSHP-10-12), the XRD patterns of the products (not shown) indicated the formation of hydrocalumite ($Ca_2Al(OH)_{6.5}Cl_{0.5}.3H_2O$), Al-tobermorite ($Ca_5Si_5Al(OH)O_{17}.5H_2O$), tobermorite 9A ($Ca_5Si_6(OH)_2O_{16}.4H_2O$), brucite ($Mg(OH)_2$) and katoite ($Ca_3Al_2(SiO_4).(OH)_8$) as the main phases. There was no influence on the crystallization time. The sample which was synthesized only by using the fusion step (CSHP-9) presented periclase, sodium hydroxide, calcium silicate, and sodium aluminate as the main phases.

The experiments carried out with the fusion step at 600 °C (by using different reaction times), with NaOH as mineralizing agent, and without the adjustment of the molar ratio (Tab. 1, CSHP-13 and CSHP-15), presented XRD patterns of the products with the predominance of CSH compounds, including tobermorite, Al-tobermorite and hydrated calcium aluminate (Fig. 4). In addition, the fusion time did not influence the final result.

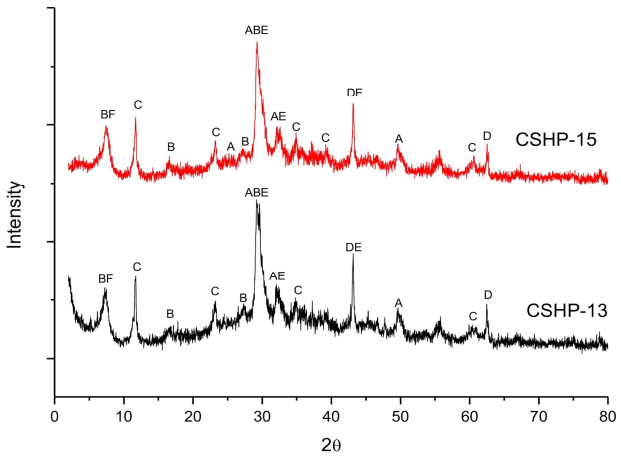

Fig. 4. XRD Patterns of the CSHP products synthesized by using the fusion step at 600 °C (A = Tobermorite 9A- $Ca_5Si_6(OH)_2O_{16}.4H_2O$, B = Al-tobermorite - $Ca_5Si_5Al(OH)O_{17}.5H_2O$, C = Hydrated magnesium aluminum hydroxide - $MgAl(OH)_{14}.H_2O$, D = Periclase - MgO, E = Hydrated calcium silicate $Ca_{1.5}SiO_{3.5}.H_2O$, and F = Sodium calcium aluminosilicate - $Na_{0.45}Ca_{0.55}Al_{1.55}Si_{2.45}O_8$).

The XRD patterns of the samples synthesized without adjustment of the molar ratios (Tab. 1, CSHP-13) and with adjustment by the addition of Ca and Si (Tab. 1, CSHP-14), did not present relevant differences between the formed phases, as shown in Fig. 5. Both samples presented tobermorite and Al-tobermorite as main phases.

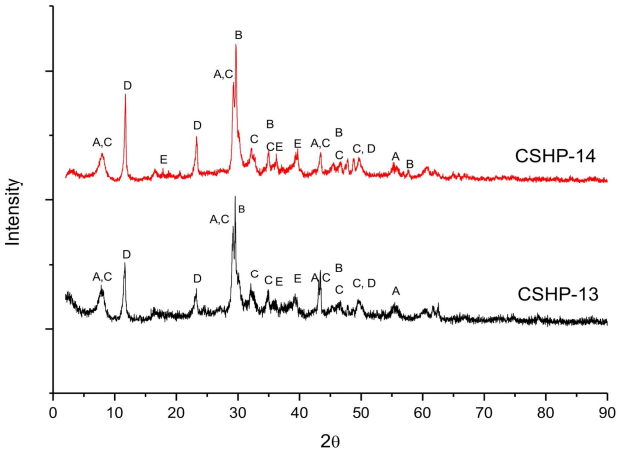

Fig. 5. XRD Patterns of the CSHP products synthesized by using the fusion step at 600 °C and with and without Ca and Si addition (A = Tobermorite 9A - $Ca_5Si_6(OH)_2O_{16}.4H_2O$, B = Al-tobermorite $Ca_5Si_5Al(OH)O_{17}.5H_2O$, C = Tobermorite - $Ca_{2.25}(Si_3O_{7.5}(OH)_{1.5})(H_2O)$, D = hydrogensilicate $H_2Si_2O_5$).

3.3 Selection of synthesized products

The products selected for the cesium adsorption studies were obtained under fusion step temperature of 600 °C for 1 h, by using NaOH as a mineralizing agent, without and with the addition of calcium and silicon (Tab. 1, CSHP-13 and CSHP-14 , respectively). These products were

selected because they presented the predominance of tobermorite and Al-tobermorite.

The determination of the cation exchange capacity (CEC) was carried out to evaluate the affinity of the synthesized materials in ions removal (Tab. 6). Sodium ions can compete with cesium ions for the active sites of the adsorbent material, thus a low CEC can indicate satisfactory cesium removal efficiency [29, 30]. CEC values between 0.12 and 0.16 meq g^{-1} for Tobermorite and between 1.28 and 1.97 meq g^{-1} for Al-Tobermorite have been reported in the literature [31]. Table 6 results indicate that both synthetic CSHP can present satisfactory cesium adsorption efficiency [29, 30].

Table 6 Cation Exchange Capacities of the synthetic CSHP

Sample	CEC (meq g^{-1})
CSHP-13	0.2359
CSHP-14	0.1707

The determination of zeta potential was evaluated by the pH changes (between 2 and 12, and varying from 1 to 1) for the CSHP-13 and CSHP-14 samples. The temperature of the tests was 25 °C. Thus, it was possible to determine the pH range where the synthesized materials have the most appropriate surface charge for the Cs^+ removal. The results are shown in Fig. 6, including the raw material (FGD) for comparison.

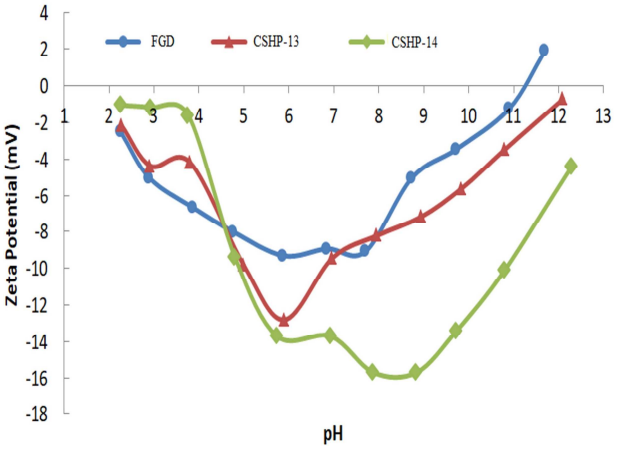

Fig. 6. Zeta potential values for the products synthesized from FGD waste.

Fig. 6 shows that the most interesting pH range for Cs^+ adsorption tests, which is where the material charge value is more negative, it is between pH 5 to 8 for the CSHP-13 sample, while CSHP-14 sample presented a wider pH working range (between 5 to 10). The synthesized products showed lower negative charges values when compared to the raw material.

3.4 Cesium adsorption studies

CSHP-14 sample was used as an adsorbent material for the removal of Cs^+ from the aqueous solution because presented less affinity for the sodium ions and higher values of negative surface charge.

3.4.1 Adsorption isotherms

The Langmuir and Freundlich models were adjusted to experimental data through the nonlinear estimation method. A plot was drawn between C_e (the equilibrium concentration of the solute in the bulk solution) versus q_e (the amount of solute adsorbed per unit weight of adsorbent at equilibrium) using the experimental and predicted value (Fig. 7). The regression coefficients for both adjustments were determined using nonlinear expression [18-19] and are shown in Tab. 7.

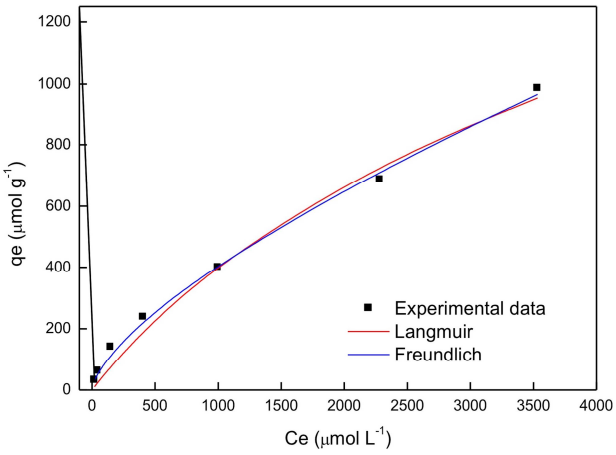

Fig. 7. Adsorption isotherm of Cs^+ onto CSHP-14.

Table 7 Parameters of isotherm models for Cs^+ onto CSHP-14.

Adsorption Isotherm Model	Parameters
Langmuir	
Q_{max} or K_L (µmol g^{-1})	1949
b (L µmol^{-1})	2.70 x 10^{-4}
R_{aj}^2	0.980
χ^2	83.9
Freundlich	
K_F [(µmol g^{-1})(L µmol $^{-1}$)$^{1/n}$]	4.06
1/n	0.669
R_{aj}^2	0.996
χ^2	9.21

Analyzing Figure 7, it can be seen that Freundlich model simulated more adequately the experimental adsorption isotherm data. Table 7 shows that the Freundlich model presented the highest value for R_{aj}^2 (coefficient of determination) and the lowest value for χ^2 (chi-square) when compared to the Langmuir model and, therefore, is the most appropriate model to describe the adsorption balance of Cs^+ onto CSHP-14. Thus, homogeneous, and heterogeneous distributions can occur by adsorption in monolayer and multilayer, in a process that can occur simultaneously or subsequently in order of time, both at random [32].

3.4.2 Adsorption study of Cs^+ in saline medium

It is a challenge to remove Cs^+ from seawater because of its low concentrations (usually between 10^{-3} to 10^{-5} mol L^{-1}) along with many other ionic species that are in high concentrations (mainly Na^+), which compete for the active sites of the adsorbent. Therefore, Cs^+ selectivity of various adsorbents can decrease significantly with high salt concentrations [2, 28, 33].

The results of Cs^+ adsorption onto CSHP-14 obtained in aqueous and saline media are shown in Tab. 8. The adsorbent material showed a high Cs^+ adsorption capacity in deionized water and a decrease of 56% and 62% in saturated media with the Na^+ ions and seawater, respectively.

Table 8 Cesium uptake by CSHP-14

	Removal (%)	q (μmol g^{-1})	k_d (mL g^{-1})
Deionized water	77.5	62.0	1381
0.02 mol L^{-1} NaCl solution	34.4	27.5	209.6
Seawater	29.5	23.6	167.6

Tobermorite substituted by aluminum has a high adsorption capacity and high selectivity for Cs^+, even when in a saturated medium with a high concentration of sodium [6]. The synthesized material is not a pure Al-tobermorite and, therefore, the mixture of materials does not present the same degree of selectivity to Cs^+ ions. However, even though the degree of selectivity of the high-purity material has not been reached, the use of material synthesized from FGD can still be viable when compared to adsorbent materials from other residues [3].

4. CONCLUSIONS

The formation of tobermorite and Al-tobermorite was identified in the products obtained from wet flue gas desulfurization waste using the alkali fusion method with NaOH. The optimal fusion temperature was 600 °C for 1 h. The required corresponding crystallization temperature was 100 °C and the crystallization time was 24 h.

The synthesized material revealed high selective uptake for Cs^+ in water. The Langmuir and Freundlich adsorption isotherms were applied to equilibrium data, and the data were found to fit the Freundlich model.

The maximum adsorption capacity of Cs^+ onto the synthesized material, as calculated from the Langmuir model, is 1949 μmol g^{-1}. It was found that the synthetic material showed a satisfactory Cs^+ removal from both deionized water and seawater. The conversion from FGD gypsum to CSH compounds shows both economic and environmental benefits when low-grade wastes are used as a valuable absorbent.

AUTHOR INFORMATION

Corresponding Author

*Email: julianaizidoro@usp.br

ORCID

Denise Alves Fungaro : 0000-0003-1618-0264

Juliana de Carvalho Izidoro : 0000-0002-3466-5196

REFERENCES

[1] Lalhmunsiama Lalhmunsiama, Kim Jae-Gyu, Choi Suk Soon, Lee Seung-Mok. Recent Advances in Adsorption Removal of Cesium from Aquatic Environment. *Applied Chemistry for Engineering.* 2018; 29(2):127-137

[2] Lee Ha Young, Kim Hu Sik, Jeong Hae-Kwon, Park Man, Chung Dong-Yong, Lee Keun-Young, Lee Eil-Hee, Lim Woo Taik. Selective Removal of Radioactive Cesium from Nuclear Waste by Zeolites: On the Origin of Cesium Selectivity Revealed by Systematic Crystallographic Studies. *The Journal of Physical Chemistry C.* 2017; 121(19)

[3] Wajima Takaashi. Synthesis of Tobermorite from the Ash after Treatment of Asbesto-Containing Disaster Waste, and Its Removal Ability of Cs(I) from Aqueous Solution. *Engineering Journal.* 2016; 20(4)

[4] Wang Jianlong, Zhuang Shuting. Removal of cesium ions from aqueous solutions using various separation technologies. *Reviews in Environmental Science and Bio/Technology.* 2019; 18(2)

[5] Zhang Hongsen, Liu Qi, Wang Jun, Liu Jingyuan, Yan Huijun, Jing Xiaoyan, Zhang Bin. Preparation of magnetic calcium silicate hydrate for the efficient removal of uranium from aqueous systems. *RSC Advances.* 2015; 5(8)

[6] Komarneni Sridhar, Komarneni Jayanth S, Newalkar Bharat, Stout Stephen. Microwave-hydrothermal synthesis of Al-substituted tobermorite from zeolites. *Materials Research Bulletin.* 2002; 37(6)

[7] Galvánková L, Bartoníčková E, Opravil T, Tkacz J, Ptáček P. The influence of starting materials´ solubility on tobermorite structure formation under the hydrothermal conditions. *IOP Conference Series: Materials Science and Engineering.* 2018; 379

[8] Galvánková Lucie, Másilko Jiří, Solný Tomáš, Štěpánková Eva. Tobermorite Synthesis Under Hydrothermal Cond tions. *Procedia Engineering.* 2016; 151

[9] Zeng Lu, Yang Ligang, Wang Shuping, Yang Kai. Synthesis and Characterization of Different Crystalline Calcium Silicate Hydrate: Application for the Removal of Aflatoxin B1 from Aqueous Solution. *Journal of Nanomaterials.* 2014; 2014

[10] Ma Weiping, Brown Paul W., Komarneni Sridhar. Sequestration of Cesium and Strontium by Tobermorite Synthesized from Fly Ashes. *Journal of the American Ceramic Society.* 1996; 79(6)

[11] Yao Zhidong, Tamura Chikashi, Matsuda Motohide, Miyake Michihiro. Resource recovery of waste incineration fly ash: Synthesis of tobermorite as ion exchanger. *Journal of Materials Research.* 1999; 14 (11)

[12] Luo Feng, Wei Cundi, Xue Bing, Wang Shujuan, Jiang Yinshan. Dynamic hydrothermal synthesis of Al-substituted 11 Å tobermorite from solid waste fly ash residue-extracted Al2O3. *Research on Chemical Intermediates.* 2012; 39(2)

[13] Córdoba Patricia. Status of Flue Gas Desulphurisation (FGD) systems from coal-fired power plants: Overview of the physic-chemical control processes of wet limestone FGDs. *Fuel.* 2015; 144

[14] Rovani Suzimara, Santos Jonnatan J., Corio Paola, Fungaro Denise A.. Highly Pure Silica Nanoparticles with High Adsorption Capacity Obtained from Sugarcane Waste Ash. *ACS Omega.* 2018; 3(3)

[15] Diamond Sidney, White Joe L., Dolch W. L.. Effects of isomorphous substitution in hydrothermally-synthesized tobermorite. *American Mineralogist.* 1966; 51(3-4_Part_1):388-401.

[16] Kalousek GEORGE L.. Crystal Chemistry of Hydrous Calcium Silicates: I, Substitution of Aluminum in Lattice of Tobermorite. *Journal of the American Ceramic Society.* 1957; 40(3)

[17] Mitsuda Takeshi. Synthesis of Tobermorite from Zeolite. *Mineralogical Journal.* 1970; 6(3)

[18] Langmuir Irving. THE ADSORPTION OF GASES ON PLANE SURFACES OF GLASS, MICA AND PLATINUM.. *Journal of the American Chemical Society.* 1918; 40(9)

[19] Freundlich H. M. F.. Over the Adsorption in Solution. *The Journal of Physical Chemistry.* 1906; 57:385-471.

[20] Ho Yuh-Shan. Selection of optimum sorption isotherm. *Carbon.* 2004; 42(10)

[21] Heebink LV, Buckley TD, Pflughoeft-Hassett DF. *A review of literature related to the use of spray dryer absorber material-production, characterization, utilization applications, barriers, and recommendations.* 2007.

[22] Laperche Valérie, Bigham Jerry M.. Quantitative, Chemical, and Mineralogical Characterization of Flue Gas Desulfurization By-Products. *Journal of Environmental Quality.* 2002; 31(3)

[23] Hansen Brian B., Kiil Søren. Investigation of Parameters Affecting Gypsum Dewatering Properties in a Wet Flue Gas Desulphurization Pilot Plant. *Industrial & Engineering Chemistry Research.* 2012; 51(30)

[24] Izidoro Juliana De Carvalho, Miranda Caio, Castanho Davi, Rossati Carlos, Campello Felipe, Guilhen Sabine, Fungaro Denise, Wang Shaobin. Physical and chemical characteristics of feed coal and its by-products from a Brazilian thermoelectric power plant. *Journal of Applied Materials and Technology.* 2019; 1(1)

[25] Mineralienatlas - Fossilienatlas. 2020.

[26] Hemmings R. T., Berry E. E.. On the Glass in Coal Fly Ashes: Recent Advances. *MRS Proceedings.* 1987; 113

[27] Kost David A., Bigham Jerry M., Stehouwer Richard C., Beeghly Joel H., Fowler Randy, Traina Samuel J., Wolfe William E., Dick Warren A.. Chemical and Physical Properties of Dry Flue Gas Desulfurization Products. *Journal of Environmental Quality.* 2005; 34 (2)

[28] Izidoro Juliana de C., Fungaro Denise A., Abbott Jennifer E., Wang Shaobin. Synthesis of zeolites X and A from fly ashes for cadmium and zinc removal from aqueous solutions in single and binary ion systems. *Fuel.* 2013; 103

[29] Johan Erni, Yamada Toshio, Munthali Moses Wazingwa, Kabwadza-Corner Ponyadira, Aono Hiromichi, Matsue Naoto. Natural Zeolites as Potential Materials for Decontamination of Radioactive Cesium. *Procedia Environmental Sciences.* 2015; 28

[30] Munthali M.W., Johan E., Aono H., Matsue N.. Cs+ and Sr2+ adsorption selectivity of zeolites in relation to radioactive decontamination. *Journal of Asian Ceramic Societies.* 2015; 3(3)

[31] Komarneni Sridhar, Roy Della M.. New tobermorite cation exchangers. *Journal of Materials Science.* 1985; 20(8)

[32] Mohd Din Azam T, Hameed Bassim H.. Adsorption of Methyl Violet Dye On Acid Modified Activated Carbon: Isotherms And Thermodynamics. *Journal of Applied Sciences in Environmental Sanitation.* 2010; 5 (2):151-160.

[33] Yang Huajun, Luo Min, Luo Li, Wang Hongxiang, Hu Dandan, Lin Jian, Wang Xiang, Wang Yanlong, Wang Shuao, Bu Xianhui, Feng Pingyun, Wu Tao. Highly Selective and Rapid Uptake of Radionuclide Cesium Based on Robust Zeolitic Chalcogenide via Stepwise Ion-Exchange Strategy. *Chemistry of Materials.* 2016; 28(23)